JOURNAL OF BACTERIOLOGY, July 2004, p. 4486–4491 Vol. 186, No. 14
0021-9193/04/$08.00+0 DOI: 10.1128/JB.186.14.4486–4491.2004

Detachment Characteristics and Oxacillin Resistance of *Staphyloccocus aureus* Biofilm Emboli in an In Vitro Catheter Infection Model

C. A. Fux,[1] S. Wilson,[1] and P. Stoodley[1,2,3]*

Center for Biofilm Engineering[1] and Departments of Mechanical Engineering and Microbiology,[2] Montana State University—Bozeman, Montana 59717, and Center for Genomic Sciences, Allegheny-Singer Research Institute, Pittsburgh, Pennsylvania 15212[3]

Received 29 October 2003/Accepted 16 January 2004

Catheter-related bloodstream infections due to *Staphylococcus aureus* are of increasing clinical importance. The pathophysiological steps leading to colonization and infection, however, are still incompletely defined. We observed growth and detachment of *S. aureus* biofilms in an in vitro catheter-infection model by using time-lapse microscopy. Biofilm emboli were characterized by their size and their susceptibility for oxacillin. Biofilm dispersal was found to be a dynamic process in which clumps of a wide range of diameters detach. Large detached clumps were highly tolerant to oxacillin compared with exponential-phase planktonic cultures. Interestingly, the degree of antibiotic tolerance in stationary-phase planktonic cultures was equal to that in the large clumps. The mechanical disruption of large clumps reduced the minimal bactericidal concentration (MBC) by more than 1,000 times. The MBC for whole biofilm effluent, consisting of particles with an average number of 20 bacteria was 3.5 times higher than the MBC for planktonic cultures. We conclude that the antibiotic resistance of detached biofilm particles depends on the embolus size and could be attributed to nutrient-limited stationary-phase physiology of cells within the clumps. We hypothesize that the detachment of multicellular clumps may explain the high rate of symptomatic metastatic infections seen with *S. aureus*.

Roughly 40% of the general population are colonized with *Staphylococcus aureus* and therefore carry an increased risk for infections associated with surgery, dialysis, or intravascular devices (11). The expanding use of invasive procedures in modern medicine has resulted in an increase of both *S. aureus* bacteremia and endocarditis, feared for their high mortality and rising rates of antibiotic resistance (16). Infected intravascular devices are a leading cause of invasive *S. aureus* infections. They accounted for 70% of the increase in hospital-acquired *S. aureus* bloodstream infections over a 10-year period in one study (20). The colonization of transcutaneous catheters from the skin flora and hub contaminants is inescapable over time and involves both the outer and inner surface of the device (18). Under continuous flow conditions, bacteria form a biofilm and eventually cause systemic infections by detached particles. In clinical experience, mechanical biofilm detachment by flushing a colonized catheter incidentally provokes sepsis. *S. aureus* bacteremia has been associated with metastatic infections in 31% of patients (13), and endocarditis has been associated with such infections in up to 25% of patients (9).

Despite their increasing clinical importance, the pathophysiological steps leading to catheter colonization and infection are incompletely defined. There is growing evidence for the impact of flow-mediated mass transport and shear forces, which are effective under almost any physiological growth condition. Their importance is highlighted by the potential to reestablish "classical" biofilm architecture in quorum-sensing knockout mutants, which form flat biofilms in static culture (17). Stoodley et al. have developed an in vitro model that allows the study of biofilm growth and dispersal under flow conditions by time-lapse microscopy (22). Detached particles of a gram-negative mixed-species biofilm were found to range from single cells up to clumps of thousands of bacteria (23). Detachment dynamics and resistance patterns of detached biofilm particles, however, have not yet been addressed.

The treatment of catheter-related infections and endocarditis is difficult and almost inevitably requires the replacement of infected foreign body material for cure (14, 16). Embolization from *S. aureus* endocarditis may persist for days after the onset of a high-dose parenteral antibiotic combination therapy. This tolerance to antimicrobial therapy and the host's immune system is based on the organization of the bacteria as a biofilm (6). Biofilm resistance has been related to restricted nutrient penetration into biofilms, leading to a metabolically dormant state of embedded bacteria (25). Other mechanisms, such as biofilm-specific quorum-sensing signals, have been proposed (8).

We hypothesized that detached clumps may preserve the antimicrobial tolerance associated with attached biofilms. The reduced antibiotic susceptibility of biofilm emboli from endocarditis vegetations or medical devices such as endovascular catheters or endotracheal tubes would thereby represent another, previously unrecognized implication of biofilm infections. Furthermore, the mechanism of antimicrobial tolerance is important when considering therapeutic strategies. If tolerance persisted after the dissolution of the clumps, it could not solely be explained by restricted diffusion into the emboli. This finding would strongly argue in favor of an additional, biofilm-specific mechanism of tolerance. The current study describes dispersal mechanisms in an *S. aureus* biofilm and quantifies

* Corresponding author. Mailing address: Center for Genomic Sciences, Allegheny-Singer Research Institute, 320 East North Ave., 11th floor, South Tower, Pittsburgh, PA 15212-4772. Phone: (412) 359-6876. Fax: (412) 359-6995. E-mail: pstoodle@wpahs.org.

embolization over time. Biofilm emboli are characterized by their size as well as their susceptibility to oxacillin, a β-lactam currently used to treat *S. aureus* infections. The increased antibiotic tolerance of biofilm emboli provides a pathophysiologic basis for the deleterious effect of *S. aureus* emboli observed in vivo.

MATERIALS AND METHODS

Bacterial strain and culture conditions. All experiments were done with *S. aureus* ATCC strain 25923. Planktonic cultures and flow cell inocula were grown in brain heart infusion (BHI) medium (Difco, Becton Dickinson, Sparks, Md.) at 37°C. The doubling time (D_t) in exponential growth was 1.57 h. Logarithmic and stationary-phase cultures were grown for 6 and 18 h, respectively. An overnight culture was used for flow cell inocula. Biofilm reactors were run with 10% BHI medium, aerated in a mixing chamber.

Biofilm reactor. Once-through systems were set up as described earlier (23). Biofilms were grown in 1- by 1-mm square, 140-mm-long glass flow cells (model FC91; BioSurface Technologies, Corp., Bozeman, Mont.) with 740-mm connective silicone tubing draining the effluent into a container. The total surface area and volume available for colonization were 85 cm^2 and 5.74 ml, respectively. The glass tube accounted for 5.5 cm^2 and 0.14 ml, and the silicone tubing accounted for 79.5 cm^2 and 5.6 ml. A 2-ml inoculum [$(7.94 \pm 3.98) \times 10^5$ CFU/ml] was injected into the inoculation port directly preceding the flow cell. Bacteria were allowed to attach for 45 min before starting a continuous flow of 1 ml min^{-1}. As the residence time within the reactor system of 5.7 min was far below D_t, we assumed that any cells found in the effluent had detached from the biofilm. The reactor's temperature was maintained at 37 ± 2°C.

Microscopy and image analysis. Biofilm dynamics within the flow cell were continuously registered with a camera (COHU 4910 series monochrome charge-coupled device) mounted on an Olympus microscope. Detached particles were analyzed by epifluorescent (Nikon) and confocal (Leica) microscopy. Images were processed with a DigitalScion VG-5 PCI framestore board and Scion Image software (Scion Image).

Biofilm surface area coverage and thickness measurements. Mean values were calculated from three independent experiments, each including daily measurements at five random locations with a ×20 objective. Biofilm thickness was assessed by measuring the stage movement in the *z* direction from the inner wall of the flow cell to the biofilm top. Refraction was corrected by multiplication by 1.36 (22).

Concentration and size distribution of detached particles. The number and size distribution of detached particles were assessed daily by filtering 1-ml aliquots of effluent onto 0.22-μm black polycarbonate membranes (Whatman Nuclepore Track-Etch membrane; Clifton, N.J.). The effluent was treated gently to minimize physical disruption of clumps. Prior to all transfers, samples were mixed by gently inverting. The detached particles were stained with LIVE/DEAD stain (*Bac*Light bacterial viability kit; Molecular Probes, Eugene, Oreg.) and observed with a ×100 oil immersion objective to determine number and size. Since the vacuum flattened the bacterial clumps onto the filter membrane, the area per clump could be correlated with the number of cells per clump, allowing automated image analysis. The degree of flattening was estimated by confocal microscopy. Monolayers were found in clumps with diameters between 8 and 32 μm, bilayers in clumps between 16 and 40 μm, and trilayers in clumps between 28 and 40 μm. The average area of a single cell was 0.774 ± 0.243 μm^2 ($n = 124$). The correlation coefficient for clumps of more than 2 cells found by linear regression was 0.951 cell/μm^2 ($r^2 = 0.96$, $n = 65$). For automated counting, particles with areas of 0.774 ± 0.243 μm^2 were counted as 1 cell and for larger particles the regression correlation was used. This assumption is conservative and probably underestimated the cell numbers of larger clumps. The software analyzed a minimum of 50 images per sample with a field area of 5,903 μm^2. Data were combined to calculate the total cell count (TCC) of the biofilm effluent.

Mechanical dispersal of detached particles. Planktonic cultures, whole effluent, and individual large clumps were homogenized to quantify their biomass and antibiotic susceptibility by colony counts. We compared three modes of homogenization: vortexing alone, sonication in a water bath (Fisher Scientific FS15) for 5 min followed by vortexing, and shear homogenization, using a Tissuemixer at 20,500 rpm (IKA Labortechnik, Wilmington, N.C.) for 30 s. Dispersed samples were transferred onto a membrane, and particle number and size were measured as described above.

Viable cell counts. Viable cell concentration and antibiotic susceptibility were assessed by counting CFU according to the drop plate method (10). Dilutions were prepared with one-fourth-strength Ringers solution (Oxoid Ltd., Basingstoke, Hampshire, England), plated onto BHI agar plates, and incubated for 24 h at 37°C. A detection limit of 7.5×10^{-3} CFU/ml was achieved by plating 1 ml of resuspended pellets spun down from the original samples. The detached cell concentration in the effluent measured by viable plate count was compared with that measured by our filter method to provide an independent cross-check of the accuracy of the automated filter counting method.

Oxacillin susceptibility testing. The minimal bactericidal concentration (MBC) for bacteria in intact and mechanically dispersed large clumps was compared with those for planktonic cultures in the exponential and stationary growth phases. MBC was defined as the lowest antibiotic concentration that caused a 3-log reduction of bacterial counts. All measurements were done on a minimum of three independent replicates. Detached clumps and exponential or stationary-phase planktonic cells were added to 50 ml of BHI medium containing serially diluted oxacillin (Sigma, St. Louis, Mo.) in concentrations from 20 mg/ml to 0.05 μg/ml. Clumps measuring 0.5 to 1 mm in diameter were individually picked from the effluent with a wide-aperture pipette tip. Half of them were disrupted by sonication, as described above, before exposure to antibiotics. Stationary-phase planktonic cells were incubated either in fresh BHI medium or spent medium, which had already been used for an overnight culture. The inoculum concentrations were $(2.0 \pm 5.62) \times 10^5$ CFU/ml for clumps (as determined in 36 similar-sized particles), $(6.76 \pm 2.24) \times 10^5$ CFU/ml for exponential-phase planktonic bacteria ($n = 3$), $(1.17 \pm 1.29) \times 10^5$ CFU/ml for stationary-phase cultures in fresh medium ($n = 9$), and $(1.15 \pm 1.91) \times 10^6$ CFU/ml in spent medium ($n = 3$). After overnight incubation at 37°C, samples were centrifuged at 5,000 rpm for 5 min. The pellets were washed twice with 3 ml of BHI broth, sonicated for 5 min, and plated for CFU measurements. Subsequently, the MIC and the MBC for bacteria in sonicated and unsonicated whole biofilm effluent (harvested on day 5) and stationary-phase planktonic cultures as well as the MIC for bacteria in sonicated and unsonicated individual large clumps (harvested on days 4 to 7) were compared. The MIC was defined as the lowest antibiotic concentration preventing visible turbidity after 20 h of incubation at 37°C. Specimens of 250 μl from sonicated and unsonicated planktonic cultures and whole effluent were added to 2.5 ml each of fresh BHI broth with 1:2 serial dilutions of oxacillin ranging from 1,000 μg/ml to 0.1 μg/ml. To compensate for the high bacterial concentrations within large clumps, the MICs for these bacteria were determined spectrophotometrically at 660 nm in 200 ml of volume. Final bacterial concentrations were $(3.39 \pm 5.01) \times 10^5$ CFU/ml for whole effluent, $(7.24 \pm 3.72) \times 10^5$ CFU/ml for planktonic cultures, and $(1.58 \pm 1.58) \times 10^5$ CFU/ml for clumps. Samples of whole effluent and planktonic cultures without turbidity were thoroughly vortexed, serially diluted, plated on BHI agar plates, and incubated for 24 h at 37°C.

Statistics. Methodological differences did not allow numerical comparison of the MICs and MBCs for large clumps with the numbers of planktonic cells and whole biofilm effluent, respectively. Unless reported otherwise data are reported as the geometric mean ± 1 standard deviation (SD). Analysis of variance was used for statistical comparisons (Minitab, version 13.3, 2000; Minitab, Inc., State College, Pa.); P values of <0.001 were considered significant.

RESULTS

Biofilm analysis. Originating from adherent single cells, the growing biofilm covered 4% ± 4% of the surface area after 1 day and increased to 49% ± 38% after 7 days (Fig. 1A). The biofilm thickness reached a steady state of 34 ± 37 μm after 4 days (Fig. 1B). The biofilm architecture was heterogeneous and consisted of discrete cell clusters separated by interstitial channels and voids (Fig. 2A). The large degree of spatial heterogeneity is reflected in the large SD of the surface area coverage and thickness measurements (Fig. 1). Time-lapse imaging revealed various dynamic phenomena. We documented four different modes of dispersal: (i) continuous growth of cell clusters, (ii) detachment and reattachment of single cells, (iii) detachment and reattachment of clumps (Fig. 2B and C); and (iv) rolling motility (online images at www.erc.montana.edu/Res-Lib99-SW/Movies/2003/03-M003_4.htm). In the latter, rolling microcolonies moved along the surface at a velocity of approximately 1 μm/min.

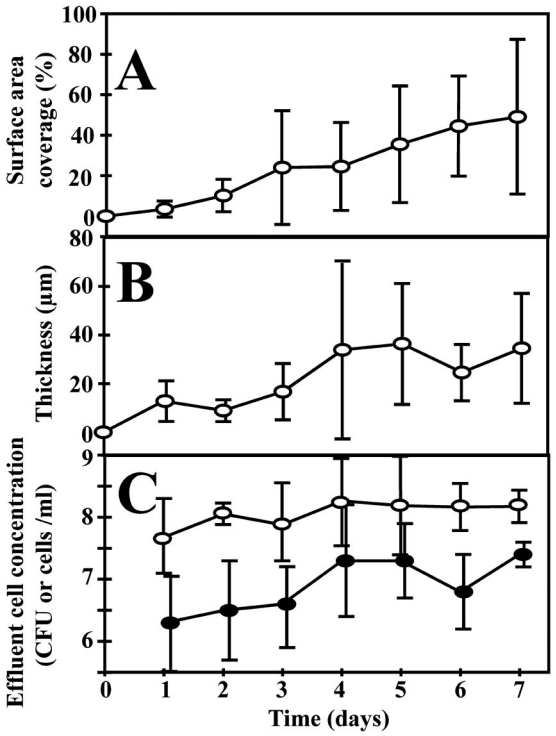

FIG. 1. Characteristics of an *S. aureus* biofilm growing in a glass flow cell. (A) Percent surface area coverage. (B) Thickness (micrometers). (C) Amount of detached biomass quantified by log total cell counts (○) and CFU per milliliter (●). Error bars represent 1 SD of the arithmetic mean (A and B) and the geometric mean (C).

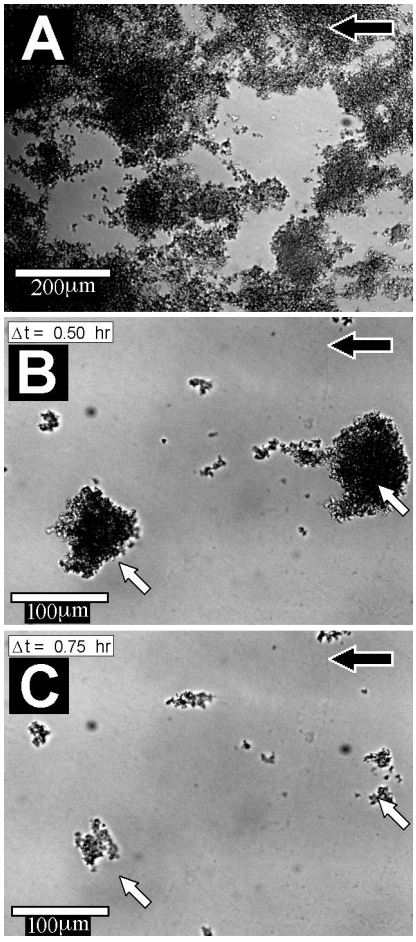

FIG. 2. Highly heterogeneous *S. aureus* biofilms. The biofilms consisted of discrete cell clusters (darker areas) separated by interstitial channels and voids (A). Time-lapse imaging documented the detachment of two large cell clusters (indicated by white arrows) from a 7-day-old biofilm over a 15-min interval (B and C). The nutrient flow direction is indicated by the black arrows. Scale bar, 100 μm.

Detachment dynamics. The daily amount of detached biomass, determined by both microscopic analysis of filtered effluent (TCC) and CFU measurements, reached a steady state after 4 days of 1.6×10^8 cells/ml and 1.6×10^7 CFU/ml respectively (Fig. 1C). During day 7, the biofilm detached a total of 3.6×10^{10} CFU per 24 h, corresponding to a detachment rate of 1.8×10^7 CFU cm^{-2} h^{-1}. The biofilm emboli captured on the filter membranes covered a wide size distribution, ranging from single cells to macroscopically visible clumps containing an estimated 10^7 bacteria (Fig. 3). Cells in the clumps were tightly packed with relatively little extracellular matrix. There was only slight daily variation in the size distribution of detached particles over the 7 days of the experiment (Fig. 3). The proportion of detached single cells ranged from 21 to 44%, contributing 7% of the detached biomass on day 7. Emboli with 11 to 100 cells accounted for 41% of particles on day 1 and 20% on day 7 and constituted the main source of detached biomass throughout the experiment (59% on day 1 and 54% on day 7). On day 7, emboli with 101 to 1,000 cells accounted for 3% of particles but 17% of detached biomass.

Mechanical disruption of detached particles. The average cell number per particle in the whole effluent was 20.1 ± 28.5, the large SD reflecting the wide size distribution of detached clumps. Shear homogenization reduced the average cell number to 5.4 ± 1.3, but sonication was the most effective homogenization strategy reducing the average cell number to 3.0 ± 0.5. CFU measurements of whole effluent reflected a similar trend in homogenization efficacy, with plate counts increasing from (3.89 ± 6.03) $\times 10^7$ CFU/ml to (8.32 ± 2.57) $\times 10^7$ CFU/ml after shear homogenization and (1.32 ± 4.17) $\times 10^8$ CFU/ml after sonication. Similarly, sonication effectively homogenized clumps with diameters between 0.5 and 1 mm from (1 ± 2.8) $\times 10^7$cells per clump to smaller aggregates with a mean of 3 ± 25 cells. Based on these results, we used sonication for further experiments.

Oxacillin susceptibility testing. MBCs for sonicated and unsonicated large clumps and planktonic cultures are shown in Fig. 4. Despite oxacillin concentrations up to 20 mg/ml, CFU of intact clumps maximally decreased from (2.0 ± 5.62) $\times 10^5$ CFU/ml ($n = 36$) to (2.34 ± 14.13) $\times 10^2$ CFU/ml ($n = 7$), thus not achieving the MBC definition. The mechanical disruption of large clumps dramatically reduced the MBC for them from >20 mg/ml ($n = 3$) to 0.8 ± 1.5 μg/ml ($n = 3$; $P < 0.001$). Bacteria in planktonic stationary phase and spent medium suffered a 1.77-log reduction at an oxacillin concentration of 0.05 μg/ml ($n = 4$) without any further effect of increasing antibiotic concentrations. In accordance with the literature, the

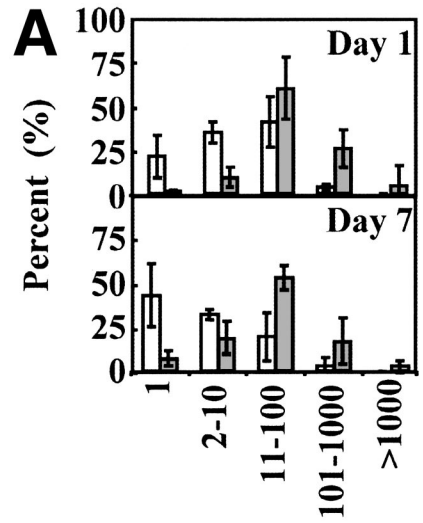

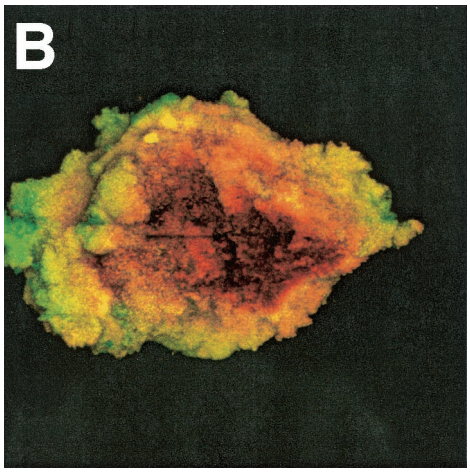

FIG. 3. Characterization of *S. aureus* biofilm emboli. (A) The size distribution of detaching particles is shown numerically (white bars) and as the total fraction of detached biomass (gray bars) for days 1 and 7. Error bars represent 1 SD. (B) Confocal image of a large clump containing ca. 10^7 CFU. Live cells (based on membrane integrity) are stained in green, and dead cells are stained in red. Field of view = 0.5 by 0.5 mm.

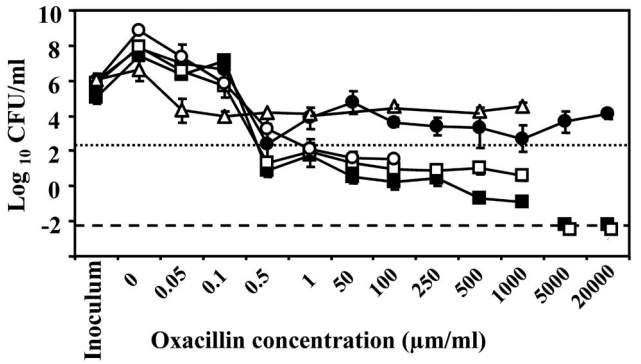

FIG. 4. Log reduction of viable cells in response to increasing oxacillin concentrations. A dotted line marks a 3-log reduction in CFU of large clumps and therefore indicates the MBC. Intact detached clumps tested in fresh medium (●) and stationary-phase planktonic cultures tested in spent medium (△) were highly tolerant to antibiotics. Mechanically disrupted large clumps (○) regained their antibiotic susceptibility. For exponential-phase planktonic cultures (□) and stationary-phase planktonic cultures in fresh medium (■), the conventional MBC was 0.5 μg/ml. A dashed line represents the detection limit. Error bars represent 1 SD.

MBCs for planktonic cells in exponential growth and stationary growth with fresh medium were 0.5 μg/ml. A significant proportion of bacteria in exponential growth survived oxacillin concentrations up to 1 mg/ml [reduction from (6.76 ± 1.29) $\times 10^5$ CFU/ml (n = 3) to 4.27 ± 2.09 CFU/ml (n = 5)], but were below the detection limit at higher concentrations. In a next step, we compared the MICs and MBCs for sonicated and unsonicated whole biofilm effluent and stationary-phase planktonic cells as well as the MIC for sonicated and unsonicated large clumps (Table 1). Contrary to the MBC measurements for large emboli, sonication did not influence the results of either planktonic cultures or whole effluent. The MICs for whole effluent (1.0 ± 2.1 μg/ml; n = 13) and planktonic cultures (0.9 ± 1.9 μg/ml; n = 9) did not differ, whereas the MBC for whole effluent (47.8 ± 2.6 μg/ml; n = 13) was significantly higher than the MBC for planktonic cultures (13.5 ± 1.2 μg/ml; n = 9; P = 0.001).

DISCUSSION

As simulated in our model, bacterial biofilms on intravascular devices are constantly exposed to flow. Flow has been shown to impose mechanical biofilm stability (21) as well as increased stress tolerance compared to bacteria in planktonic growth (26). Biofilms in a flow system are not a homogeneous layer continuously spreading downstream, but express a high degree of structural variability (Fig. 2A). This heterogeneity is stimulated by several concomitant dispersal mechanisms, with detachment and reattachment, rolling, and continuous clonal growth, all influenced by shear forces. Biofilm detached either directly from the surface, leaving bare spots, or from other bacteria, leaving behind an attached layer of cells (Fig. 2B and C).

There was a wide size distribution of detached particles from the *S. aureus* biofilm throughout the course of the experiment

TABLE 1. MIC and MBC for bacteria in whole biofilm effluent, planktonic cultures, and detached large clumps

Cells	MIC (μg/ml)		MBC (μg/ml)[b]	
	Unsonicated	Sonicated	Unsonicated	Sonicated
Whole biofilm effluent	1.0 ± 2.1	1.1 ± 1.6	47.8 ± 2.6	53.0 ± 2.1
Planktonic culture	0.9 ± 1.9	1.0 ± 1.9	13.5 ± 1.2*	13.5 ± 2.0*
Detached large clumps[a]	0.4 ± 0.0	0.3 ± 0.1	>20,000	0.8 ± 1.5**

[a] Values for detached large clumps cannot numerically be compared to whole effluent and planktonic cultures due to differences in test methodology (see Materials and Methods).

[b] *, P = 0.001 comparing MBC for whole biofilm effluent and planktonic culture; **, $P < 0.001$ comparing MBC for sonicated and unsonicated detached large clumps.

(Fig. 1C and 3). The greatest proportion of detached biomass was contributed by clumps containing between 11 and 100 cells. However, the proportion of total detached particles was more evenly distributed between single cells, clumps of 2 to 10 cells, and clumps of 11 to 100 cells. These detachment patterns sharply contrast with those of *Pseudomonas aeruginosa* biofilms (27). Whereas *P. aeruginosa* strains detach 50 to 80% single cells but only 1 to 3% particles larger than 10 cells, *S. aureus* strains detach 18 to 44% single cells and 23 to 45% emboli containing more than 10 cells. Differences between the two species suggest that there may be distinct detachment control mechanisms. There is growing evidence that detachment not only occurs passively due to hydrodynamic forces (22), but also occurs as an active process in response to population density (19), changes in substrate concentration (5), or exposure to antimicrobials (7). Involved strategies include the dissolution of extracellular polysaccharide substances through secreted enzymes or the down-regulation of surface-associated binding sites (3, 12).

The clinical relevance of species-specific dispersal characteristics is yet unknown. However, we hypothesize that the detachment of multicellular clumps may explain the high rate of symptomatic metastatic infections seen with *S. aureus*. In analogy to biofilms, antibiotic tolerance may impair embolus clearance. Despite the administration of in vivo unachievable high antibiotic concentrations, no 3-log reduction of CFU could be reached in intact clumps (Fig. 4). This is similar to MBC measurements in *S. aureus* biofilms, which exceeded the MBC for bacteria in logarithmic growth by up to 1,000 times (4). Antibiotic tolerance of biofilm emboli can explain the persistence of positive venous blood cultures observed in *S. aureus* endocarditis even days after the onset of treatment.

Interestingly, we observed a similar degree of tolerance in stationary-phase planktonic growth tested in spent medium instead of the conventionally used fresh medium for the MBC assay (Fig. 4). Upon the addition of fresh medium, bacteria restored antibiotic susceptibility comparable to that of exponential-growth-phase cultures, suggesting a direct correlation between nutritional supply, metabolic activity, and antibiotic susceptibility. This correlation is of elementary clinical significance. As diagnostic laboratories determine antibiotic resistance (MIC) and tolerance (MBC) in the logarithmic growth phase, in vitro results may not correlate with in vivo efficacy against growth-limited bacteria. This is particularly true for β-lactams, whose activity is restricted to proliferating cells (24). The similar antibiotic tolerance observed in large biofilm emboli and stationary-phase planktonic cultures suggests that starvation-induced dormancy was the common underlying mechanism for protection. The mechanical disruption of large clumps—and thereby the elimination of diffusion barriers—accordingly restored antibiotic susceptibility. The observation of starved cells in the bottom layers of a biofilm remaining unaffected by freely penetrating antibiotics further supports this interpretation (1, 2). As an alternative, the disruption of a detached clump may result in the dilution of accumulated quorum-sensing signals, which mediated metabolic inactivity and antibiotic resistance within an embolus. In this case, however, one might expect some effect of sonicating the whole biofilm effluent with its average of 20 cells per detached particle. Remarkably, the 3.5-times-higher MBC for whole effluent compared to stationary-growth-phase planktonic cultures (Table 1) resisted both sonication and the exposure to fresh medium. This increase in antibiotic tolerance may be attributed to cellular adaptations, such as the induction of stress response proteins (15).

The MIC for whole effluent did not surmount the values for planktonic bacteria, which concurs with the biofilm literature (4). However, conventional MIC testing based on optical density, as performed in this study, is more reflective of the prevention of growth of planktonic bacteria shed from the biofilm than of cell growth within the biofilm. Because of the slow growth dynamics of an established biofilm, the effect of antibiotics on growth within a biofilm can hardly be determined.

Taken together, our data suggest that the antibiotic resistance of biofilm emboli is size dependent and is mainly due to metabolic inactivity secondary to restricted diffusion. Alternative, biofilm-specific resistance mechanisms seem to play a minor role. β-Lactam therapy can be expected to clear the vast majority of biofilm emboli, but fails to sterilize larger clumps. Our data correlate with the clinical experience that acute exacerbations of *S. aureus* biofilm infections quickly respond to therapy, but metastatic infections may develop under treatment. Future research is required to characterize detachment patterns of different species under various growth conditions, as they may predict the virulence of biofilm emboli. A better understanding of detachment mechanisms may help to prevent large, antibiotic-resistant emboli.

ACKNOWLEDGMENTS

This work was supported by the National Institutes of Health RO1 grant GM60052-02 (P.S.) and the Swiss National Science Foundation grant 81BE-69256 (C.F.).

From the Center for Biofilm Engineering, we thank M. Hamilton for advice on statistical analysis and Kimberley White, 2001 Research Education for Undergraduates Program, for experimental assistance.

REFERENCES

1. **Anderl, J. N., M. J. Franklin, and P. S. Stewart.** 2000. Role of antibiotic penetration limitation in *Klebsiella pneumoniae* biofilm resistance to ampicillin and ciprofloxacin. Antimicrob. Agents Chemother. **44:**1818–1824.
2. **Anderl, J. N., J. Zahller, F. Roe, and P. S. Stewart.** 2003. Role of nutrient limitation and stationary-phase existence in *Klebsiella pneumoniae* biofilm resistance to ampicillin and ciprofloxacin. Antimicrob. Agents Chemother. **47:**1251–1256.
3. **Boyd, A., and A. M. Chakrabarty.** 1994. Role of alginate lyase in cell detachment of *Pseudomonas aeruginosa*. Appl. Environ. Microbiol. **60:**2355–2359.
4. **Ceri, H., M. E. Olson, C. Stremick, R. R. Read, D. Morck, and A. Buret.** 1999. The Calgary Biofilm Device: new technology for rapid determination of antibiotic susceptibilities of bacterial biofilms. J. Clin. Microbiol. **37:**1771–1776.
5. **Characklis, W.** 1990. Biofilm processes, p. 195–232. *In* W. G. Characklis and K. C. Marshall (ed.), Biofilms. John Wiley & Sons, New York, N.Y.
6. **Costerton, J. W., P. S. Stewart, and E. P. Greenberg.** 1999. Bacterial biofilms: a common cause of persistent infections. Science **284:**1318–1322.
7. **Daly, B., W. B. Betts, A. P. Brown, and J. G. O'Neill.** 1998. Bacterial loss from biofilms exposed to free chlorine. Microbios **96:**7–21.
8. **Davies, D. G., M. R. Parsek, J. P. Pearson, B. H. Iglewski, J. W. Costerton, and E. P. Greenberg.** 1998. The involvement of cell-to-cell signals in the development of a bacterial biofilm. Science **280:**295–298.
9. **Fowler, V. G., Jr., J. Li, G. R. Corey, J. Boley, K. A. Marr, A. K. Gopal, L. K. Kong, G. Gottlieb, C. L. Donovan, D. J. Sexton, and T. Ryan.** 1997. Role of echocardiography in evaluation of patients with Staphylococcus aureus bacteremia: experience in 103 patients. J. Am. Coll. Cardiol. **30:**1072–1078.
10. **Herigstad, B., M. Hamilton, and J. Heersink.** 2001. How to optimize the drop plate method for enumerating bacteria. J. Microbiol. Methods **44:**121–129.
11. **Kluytmans, J., A. van Belkum, and H. Verbrugh.** 1997. Nasal carriage of *Staphylococcus aureus*: epidemiology, underlying mechanisms, and associated risks. Clin. Microbiol. Rev. **10:**505–520.

12. **Lee, S. F., Y. H. Li, and G. H. Bowden.** 1996. Detachment of *Streptococcus mutans* biofilm cells by an endogenous enzymatic activity. Infect. Immun. **64:**1035–1058.
13. **Lowy, F. D.** 1998. Staphylococcus aureus infections. N. Engl. J. Med. **339:** 520–532.
14. **Mermel, L. A., B. M. Farr, R. J. Sherertz, I. I. Raad, N. O'Grady, J. S. Harris, and D. E. Craven.** 2001. Guidelines for the management of intravascular catheter-related infections. Clin. Infect. Dis. **32:**1249–1272.
15. **Novick, R. P.** 2003. Autoinduction and signal transduction in the regulation of staphylococcal virulence. Mol. Microbiol. **48:**1429–1449.
16. **Petti, C. A., and V. G. Fowler, Jr.** 2002. Staphylococcus aureus bacteremia and endocarditis. Infect. Dis. Clin N. Am. **16:**413–435, x-xi.
17. **Purevdorj, B., J. W. Costerton, and P. Stoodley.** 2002. Influence of hydrodynamics and cell signaling on the structure and behavior of *Pseudomonas aeruginosa* biofilms. Appl. Environ. Microbiol. **68:**4457–4464.
18. **Raad, I., W. Costerton, U. Sabharwal, M. Sacilowski, E. Anaissie, and G. P. Bodey.** 1993. Ultrastructural analysis of indwelling vascular catheters: a quantitative relationship between luminal colonization and duration of placement. J. Infect. Dis. **168:**400–407.
19. **Sauer, K., A. K. Camper, G. D. Ehrlich, J. W. Costerton, and D. G. Davies.** 2002. *Pseudomonas aeruginosa* displays multiple phenotypes during development as a biofilm. J. Bacteriol. **184:**1140–1154.
20. **Steinberg, J. P., C. C. Clark, and B. O. Hackman.** 1996. Nosocomial and community-acquired Staphylococcus aureus bacteremias from 1980 to 1993: impact of intravascular devices and methicillin resistance. Clin. Infect. Dis. **23:**255–259.
21. **Stoodley, P., R. Cargo, C. J. Rupp, S. Wilson, and I. Klapper.** 2002. Biofilm material properties as related to shear-induced deformation and detachment phenomena. J. Ind. Microbiol. Biotechnol. **29:**361–367.
22. **Stoodley, P., L. Hall-Stoodley, and H. M. Lappin-Scott.** 2001. Detachment, surface migration, and other dynamic behavior in bacterial biofilms revealed by digital time-lapse imaging. Methods Enzymol. **337:**306–319.
23. **Stoodley, P., S. Wilson, L. Hall-Stoodley, J. D. Boyle, H. M. Lappin-Scott, and J. W. Costerton.** 2001. Growth and detachment of cell clusters from mature mixed-species biofilms. Appl. Environ. Microbiol. **67:**5608–5613.
24. **Tuomanen, E., R. Cozens, W. Tosch, O. Zak, and A. Tomasz.** 1986. The rate of killing of Escherichia coli by beta-lactam antibiotics is strictly proportional to the rate of bacterial growth. J. Gen. Microbiol. **132:**1297–1304.
25. **Walters, M. C., III, F. Roe, A. Bugnicourt, M. J. Franklin, and P. S. Stewart.** 2003. Contributions of antibiotic penetration, oxygen limitation, and low metabolic activity to tolerance of *Pseudomonas aeruginosa* biofilms to ciprofloxacin and tobramycin. Antimicrob. Agents Chemother. **47:**317–323.
26. **Wilson, J. W., C. M. Ott, R. Ramamurthy, S. Porwollik, M. McClelland, D. L. Pierson, and C. A. Nickerson.** 2002. Low-shear modeled microgravity alters the *Salmonella enterica* serovar Typhimurium stress response in an RpoS-independent manner. Appl. Environ. Microbiol. **68:**5408–5416.
27. **Wilson, S., M. A. Hamilton, G. C. Hamilton, M. R. Shurmann, and P. Stoodley.** Statistical quantification of the detachment rates and size distribution of cell clumps from wild type (PAO1) and cell signaling mutant (JP1) *Pseudomonas aeruginosa* biofilms. Appl. Environ. Microbiol., in press.